Thermosensitive polymer-coated plasmonic nanostructures for reversible confinement biomolecules

Nguyen Thi Tuyet Mai, Claire Mangeney, Nordin Felidj

Thermosensitive polymer-coated plasmonic nanostructures for reversible confinement biomolecules

Nguyen Thi Tuyet Mai,§ Claire Mangeney,¥ Nordin Felidj¥
§University of Science and Technology of Hanoi, Vietnam Academy of Science and Technolgy, 18 Hoang Quoc Viet, Cau Giay, Ha Noi, Viet Nam.
¥University Paris Diderot - France

1 INTRODUCTION

Biomedical applications of stimuli-responsive surfaces started attracting interest in the 1980s, particularly on the basis of work by the group of Hoffman [1]. Bio-interfaces with stimuli-responsive/switchable bio-affinity have been of considerable recent research interest. The use of switchable surfaces has been discussed for cell culture, drug delivery and tissue engineering [2-5]. These surfaces are typically prepared by grafting environmentally sensitive macromolecules onto a substrate, where the type of macromolecule and substrate are chosen depending on the intended use of the surface. A typical molecule used for this purpose is poly(N-isopropylacrylamide) (PNIPAM), which is hydrated and hydrophilic below the lower critical solution temperature (LCST) in the physiologically relevant range at 32^{o}C, but above the LCST, the polymer segments are thought to become more hydrophobic. This temperature-dependent hydrophobicity transition has been exploited to selectively switch the interfacial properties of PNIPAM and its consequent interactions with cells and biomolecules [6, 7]. The change in hydration of the PNIPAM renders the PNIPAM surface adhesive or non-adhesive to bio-molecular [8-12].

Adhesion between particles of sizes in the micron to nanometer range and solid surfaces is a key factor in many industrial applications. Hardly any real surface is smooth at a submicroscopic level and practical surfaces often

possess significant roughness or are nanostructured for specific applications such as biomaterials, tissue engineering and cell cultures [13]. Surface roughness or structuration play an important role in adhesion since it reduces the contact area between the bodies leading to significantly reduced interaction. Surfaces may possess features in several length scales, but due to the short range of the van der Waals interaction, structuration in nanoscale ultimately determines the strength of adhesion. Invention and progress of colloidal probe technique have boosted the studies of adhesion and the effects of nanoscale nanostructuration or roughness. Recent studies have quantified the relative importance of the geometry, surface roughness and medium properties on the adhesion of the approaching bodies as their sizes are scaled from micro- to nano-scale.

In this work, we describe design and preparing of novel systems including plasmonic nanostructures coated by PNIPAM brushes as smart platforms for bio-particles reversible confinement. The combination of lithographic gold nanostructures and thermoresponsive polymer brushes leads to a new generation of hybrid gold/polymer system for efficiently switched from bio-adherent to bio-repellent by convenient temperature stimuli.

2 EXPERIMENTAL

2.1 Materials

Reagent grade solvents were purchased from VWRProlabo and Alfa Aesar. 2-Bromopropionyl bromide (BPB) (97%, Aldrich), triethylamine (TEA) (99%, Merck), CuBr (98%, Sigma-Aldrich), N,N,N′,N″,N″-pentamethyldiethyltriamine (PMDETA) (99%, Acros Organics) were used as received. N-Isoproylacrylamide (NIPAM) (99%, Acros Organics) was purified by recrystallization in n-hexane solution. Bovine Serum Albumin (BSA) 98% was obtained from Sigma-Aldrich.

2.2 Elaboration of gold nanostructures array

Golf nanoparticles arrays are fabricated by electron beam lithography (EBL). The starting point is a flat substrate that is conducting to prevent charging. For optical applications, ITO covered glass plates have become widely used. The substrate is spin coated with an electron sensitive resist, typically 90 nm thick. Resists as polymethylmethacrylate (PMMA) consist of macromolecules that are modified upon exposure to high-energy electrons, resulting in a changed solubility. A desired sample pattern can thus be transferred to the resist by writing the pattern with an electron beam and subsequent wet chemical development. The resulting patterned resist layer serves as a mask for depositing the sample material by vacuum evaporation. Finally, a lift-off step removes the resist mask and excess material on top of it, leaving the sample structures on the surface.

2.3 Functionalization of gold nanostructures by PNIPAM brushes

2.3.1 Synthesis of diazonium salt:

The 4-Hydroxyethylbenzene Diazonium Tetrafluoroborate Salt ($+N_2$-C_6H_4-CH_2-CH_2-OH) was synthesized following this protocol: A stirred solution of 2-(4-aminophenyl)ethanol (0.69 g) and HBF4 (1.8 mL) in acetonitrile (3 mL) at −10 °C was added dropwise to a solution of tert-butylnitrite (0.63 g) in acetonitrile (3 mL) at −10 °C. The resulting mixture was kept overnight at −10 °C. The precipitate was washed three times with 50 mL of diethyl ether, then with 50 mL of acetone, and finally evaporated under vacuum. The 4-(2-hydroxyethyl)benzene diazonium tetrafluoroborate salt was stored at −10 °C.

2.3.2 Initiator-modified gold surfaces:

The atom transfer radical polymerization initiator was grafted in 2 steps. *(i)* Spontaneous grafting of 4–hydroxyethylbenzene diazonium tetrafluoroborate salt (0.003 M) was achieved on cleaned gold nanostructures array by incubation for 6h at room temperature. *(ii)* Then, the terminal hydroxyl groups were treated with 2-bromoisobutyryl bromide (0.1 M, toluene) in the presence of TEA (0.12 M) for 5 min to produce bromo-terminated ester groups.

2.3.3 Atomic Transfer Radical Polymerization (ATRP) of NIPAM:

Solutions were prepared and kept at room temperature during degassing by passing a continuous stream of argon through the solution while being stirred. The polymerization solution was prepared by adding a solution of an organometallic catalyst to a solution of NIPAM monomer. The extremely oxygen sensitive organometallic catalyst was prepared by adding a 5 mL solution of PMDETA in MeOH (200 μL, 1 mmol) to 30 mg of CuBr (0.2 mmol). A 3 mL portion of the resulting green solution (which could possibly turn blue due to presence of $CuBr_2$ and provide unsuccessful ATRP) was added to a solution of NIPAM monomer (2 g, 18 mmol) in 11 mL of deionized water under a continuous stream of argon. The polymerization solution was allowed to stir during degassing for 15 min and then transferred into a flask containing the initiator-modified gold surface. The resulting solution was allowed to stir at room temperature under argon for 20 min. Substrates were then removed from the flask and rinsed thoroughly with ethanol and water and subsequently dried under a flush of argon.

2.4 Instrumentation

AFM in air was performed on Nanoscope III digital instrument microscope in tapping mode to map the morphology. AFM images were processed and analyzed using the application WSxM and FabViewer. The extinction spectra were recorded by far-field extinction micro–spectroscopy in the 500-1000 nm range. The spectrometer is coupled to an upright optical microscope equipped with a 50× (Olympus, numerical aperture NA=0.35) and 100× (Olympus, NA: 0.8) objectives for experiments in air. Extinction spectra recorded in water at various temperatures used 100× immersion objective (Olympus, N.A: 1)

3 RESULTS AND DISCUSSION

3.1 Characterization PNIPAM-coated gold nanodots

GNDs array is fabricated by electron beam lithography (EBL) on an ITO-covered glass substrate with a diameter of ~220 nm and a height of 50 nm (see Fig. 1). A strong extinction of this array emerges at 600 nm in air due to excitation of LSP (Fig. 2.2c - black line). The pNIPAM brushes were grafted on the GNDs array by using our multi-step strategy (described in Fig. 2). The stepwise strategy for the preparation of the hybrid plasmonic system GND@pNIPAM consists in three major steps: (i) The spontaneous grafting of the aryl group derived from 4-hydroxyethylbenzene diazonium tetra-fluorborate salt (HEBDT) to produce –OH terminated aryl moieties, covalently anchored to the surface; (ii) Esterification of the anchored –OH groups with 2–bromoisobutyryl bromide leading to bromo-terminated gold surface which allows to initiate the Atomic Transfer Radical Polymerization (ATRP) and (iii) The grafting of pNIPAM brushes from the surface via surface-initiated ATRP.

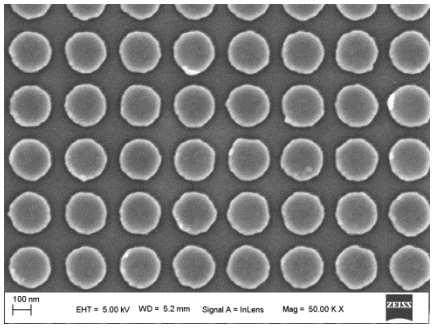

Figure 1. SEM image of gold nanodots array

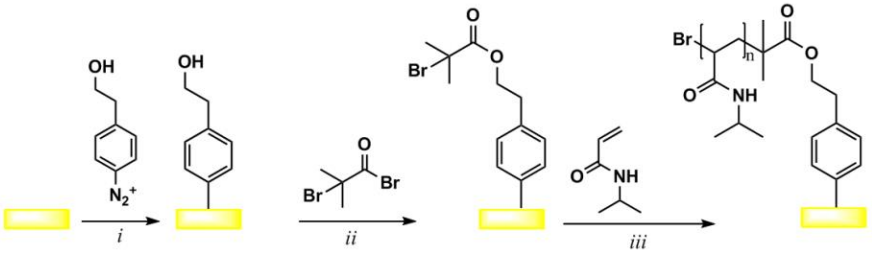

Figure 2. General scheme summarizing the stepwise strategy for the functionalization of the GNDs array: (i) spontaneous grafting of hydroxethyl–aryl groups; (ii) esterification with 2-bromoisobutyryl bromide; (iii) SI–ATRP of N–isopropylacrylamide.

The thickness of PNIPAM grafted on GNDs array was measured by AFM in air at room temperature. The AFM images of GNDs before and after grafting of PNIPAM allow estimating the dry PNIPAM thickness which is around h_{dry} ~10 ±2 nm (in air at room temperature, PNIPAM adopts a collapsed conformation), see Fig. 3a,b. In water at room temperature (below the LCST), the PNIPAM adopts a swollen conformation. The swelling ratio defined as $\alpha = h_{swollen}/h_{dry}$ (where $h_{swollen}$ and h_{dry} corresponds to the swollen and dry brush thickness) was deduced from our report to $\alpha \sim 2$ [14, 15]. Thus, the PNIPAM thickness in the swollen state can be deduced to ~ 20 ±2 nm. Increasing the external temperature up to 40°C in water (above the LCST of PNIPAM) induces a dramatic change of the polymer conformation of which the thickness significantly decreases upon heating to, 10 ±2 nm. The extinction spectra of GNDs array before and after the polymerization process indicate a red-shift of 35 nm of the LSPR wavelength (Fig. 3c). This red-shift is attributed to an increase of the local refractive index around the GNDs in presence of the polymeric layer.

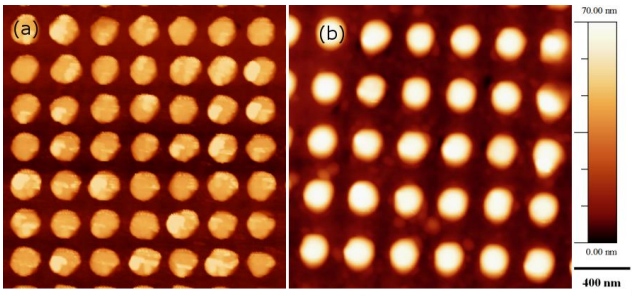

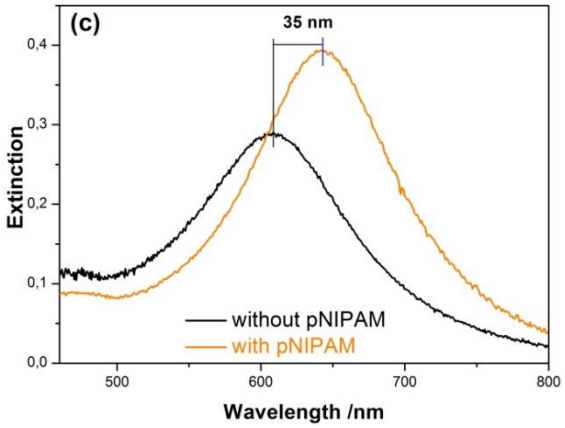

Figure 3. AFM images of GNDs (a) and GND@pNIPAM array (b). Extinction spectra in air of GNDs array before (after grafting of initiator groups)-black line and after polymerization-orange line (c).

Interestingly, when the GND@pNIPAM array is immersed in water and heated from 20 °C (below the LCST) to 40 °C (above the LCST), a red-shift of 8 nm of the LSPR wavelength is observed, as shown in Fig. 4. This red-shift is attributed to the collapse of the polymer brushes above the LCST, leading to an increase of both the polymer density close to the NPs and the refractive index of the surrounding medium. Note that the stability of our system has been checked through 6 cycles in temperature, indicating that the links between all of the components are strong, therefore making our plasmonic device very stable (inset Fig. 4).

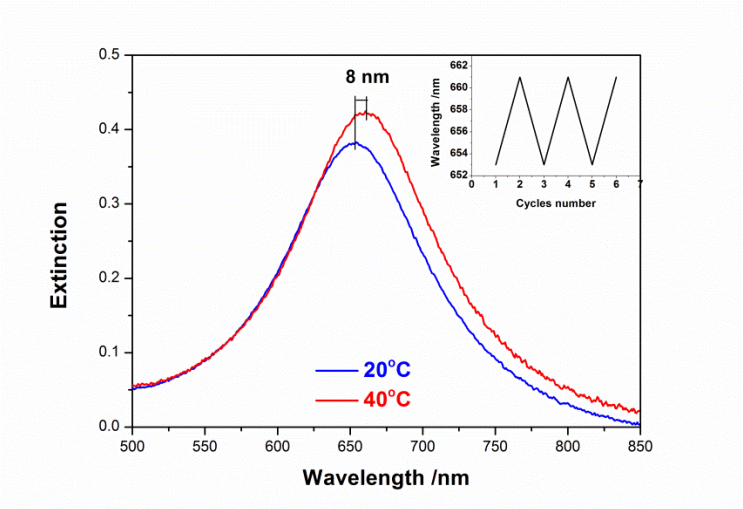

Figure 4. Extinction spectra of GND@pNIPAM recorded in water at 20 °C (blue line) and 40 °C (red line). Inset: Variation of the LSP wavelength of the GND@pNIPAM array in water as a function of the external temperature for repeated temperature cycles 20 °C and 40 °C.

3.2 Confinement of protein on the PNIPAM-grafted gold nanostructured surface

As ready mentioned, pNIPAM brushes are hydrated below the LCST of 32 °C, while above the LCST, the polymer segments become more hydrophobic. The change in hydration of the pNIPAM renders the pNIPAM surface adhesive or non-adhesive to bio-molecules. In order to investigate this behavior, we considered the thermo-controlled adsorption on GND@pNIPAM of a model protein, the Bovine Serum Albumin (BSA). The dry grafted pNIPAM thickness was h_{dry} ~ 10 nm. It is known that the hydrophobic interaction has a major role in protein adsorption phenomena. When the temperature increases above the LCST, the surface becomes more hydrophobic. Therefore, the polymer brushes collapse and are susceptible to adhere larger amounts of protein. By using the plasmonic GNDs array

structures, the adsorption of BSA as a function of temperature of the incubation procedure can be monitored by the modification of UV-vis spectra. Adsorption of BSA on GND@pNIPAM substrate was carried out by incubation of the substrate in the aqueous solution of BSA 10^{-2} M at 20 °C and 50 °C for 2h. The substrate then was rinsed by water at the same temperature (20 °C or 50 °C), dried by nitrogen gas and characterized by UV-vis absorption spectrometer. Fig. 5 displays the extinction spectra recorded in air at room temperature of GND@pNIPAM before (black curve) and after incubation in a BSA solution at 20 °C (green curve) and 50 °C (red curve). These results show that the LSP shift is negligible when the sample was incubated in BSA solution at 20 °C. In contrast, a red shift of the LSP wavelength $\Delta\lambda$ ~ 12 nm is observed after incubation the sample in the BSA solution at 50 °C. This can be attributed to the adsorbed protein on the polymer brushes which increases of the refractive index of the surrounding medium of GNDs. It to note that in the absence of BSA solution, the plasmon band of GNDs is not changed after the same experiment procedure.

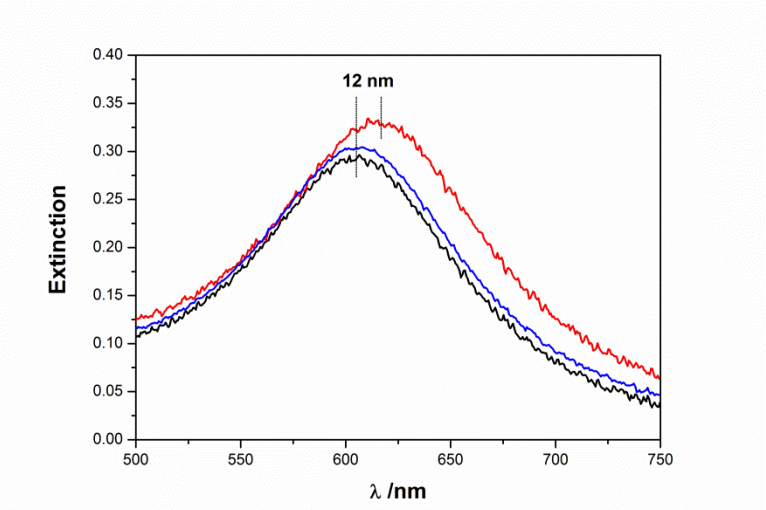

Figure 5. Extinction spectra recorded in air at room temperature of GND@pNIPAM nanostructure before (black curve) and after incubation in the BSA solution at 20 °C (blue curve) and at 50 °C (red curve).

The desorption of BSA from pNIPAM brushes was carried out by immersion of the sample (after BSA adsorption at 50 °C) in water at 20 °C. Then, the sample was rinsed in water at 20 °C and dried by nitrogen gas. Fig. 6 shows the evolution of extinction spectra of GND@pNIPAM as a function of desorption procedure time. A blue-shift of LSP wavelength is observed versus the time of immersion of the sample in water at 20 °C due to a decrease of the refractive index of the surrounding medium caused by the desorption BSA molecules from the polymer brushes. Nevertheless, we can observe that by incubating the sample in water at 20 °C for one day, the extinction spectrum couldn't be restored to the initial spectrum of nanostructure before BSA adsorption. This observation indicated that some BSA molecules still remain robustly adsorbed to the gold nanostructure substrate or insertion into the polymer brushes. In fact, the metallic nanostructures which are rough can provide several sites for proteins adsorption on its surface.

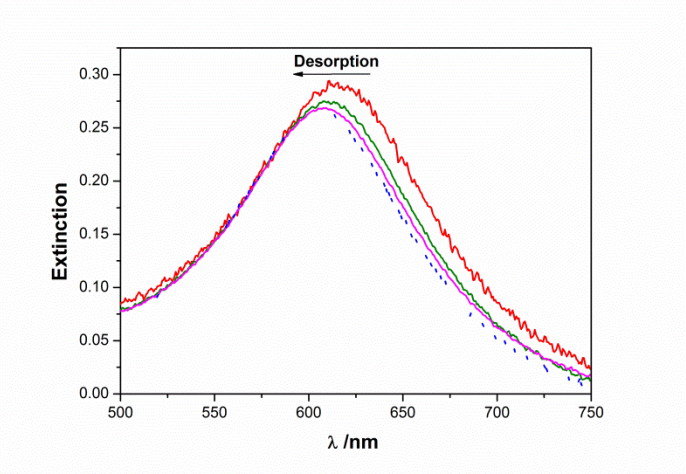

Figure 6. Extinction spectra of GND@pNIPAM with adhered BSA protein (red curve) after immersion in water 20 °C for 10 min (green curve) and 60 min (pink curve) (all spectra were recorded in air at room temperature). The pink curve is close to the blue

dashed curve - extinction spectrum of GND@pNIPAM array after incubation in BSA adsorption at 20 °C.

To verify our hypotheses, the process of thermo-induced adsorption/desorption of BSA molecules was done several times. The experimental results were shown in Fig. 7. For the first cycle, when the temperature decreased, the LSP wavelength couldn't be restored to the initial position before the BSA adsorption because several BSA molecules were trapped as mentioned above. However, from the second cycle, the shift of LSP wavelength of nanostructure becomes reversible and reproducible. Thus, the hybrid structures including GNPs and pNIPAM can be efficiently switched from bio-adherent to bio-repellent by convenient temperature stimuli.

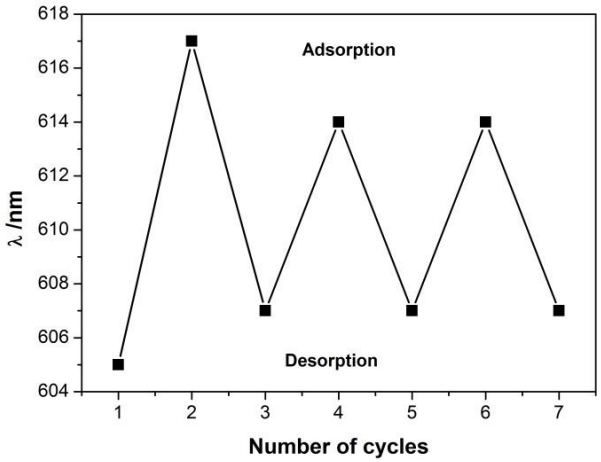

Figure 7. Variation of the LSP wavelength of GNP@pNIPAM array recorded in air as a function of adsorption/desorption cycles of BSA molecules.

4 CONCLUSION

In conlusion, we showed two examples of possible perspectives of the confinement of latex particles and protein on the hybrid thermosensitive plasmonic nanostructures GNP@pNIPAM. The temperature-dependent hydrophobic/hybrophilic property of pNIPAM was exploited to switch the adsorption/desorption of a protein bovine serum albumin. With the above characteristics, this hybrid nanostructures can be used in biomedical and biological applications such as enzyme immobilization, cell sorting, protein adsorption and purification.

References

1. Hoffman, A. S. (1987). Applications of thermally reversible polymers and hydrogels in therapeutics and diagnostics, *Journal of Controlled Release*, **6,** pp. 297-305.
2. Kikuchi, A. andOkano, T. (2002). Pulsatile drug release control using hydrogels, *Advanced Drug Delivery Reviews*, **54,** pp. 53-77.
3. Jagur-Grodzinski, J. (2006). Polymers for tissue engineering, medical devices, and regenerative medicine. Concise general review of recent studies, *POLYMERS FOR ADVANCED TECHNOLOGIES*, **17,** pp. 395–418.
4. Gupta, P., Vermani, K., andGarg, S. (2002). Hydrogels: from controlled release to pH-responsive drug delivery, *Drug Discovery Today*, **7,** pp. 569-579.
5. Robert Langer, N. A. P. (2003). Advances in Biomaterials, Drug Delivery, and Bionanotechnology, *AIChE Journal*, **49,** pp. 2990–3006.
6. Xu, F. J. (2004). Surface-Active and Stimuli-Responsive Polymer−Si(100) Hybrids from Surface-Initiated Atom Transfer Radical Polymerization for Control of Cell Adhesion, *Biomacromolecules*, **5,** pp. 2392-2403.
7. Akiyama, Y. (2004). Ultrathin Poly(N-isopropylacrylamide) Grafted Layer on Polystyrene Surfaces for Cell Adhesion/Detachment Control, *Langmuir*, **20,** pp. 5506-5511.
8. Ma H, H. J., Stiller P, Chilkoti A (2004). ''non-fouling'' oligo(ethylene glycol)-functionalized polymer brushes synthesized by surface-initiated atom transfer radical polymerization, *Advanced Materials*, **16,** pp. 338–341.
9. Gautrot, J. E. (2010). Exploiting the superior protein resistance of polymer brushes to control single cell adhesion and polarisation at the micron scale, *Biomaterials*, **31,** pp. 5030-5041.
10. Azioune, A. (2009). Simple and rapid process for single cell micro-patterning, *Lab on a Chip*, **9,** pp. 1640-1642.
11. Patel, N. G. (2012). Rapid cell sheet detachment using spin-coated pNIPAAm films retained on surfaces by an aminopropyltriethoxysilane network, *Acta Biomaterialia*, **8,** pp. 2559-2567.
12. Kumashiro, Y. (2013). Modulation of cell adhesion and detachment on thermo-responsive polymeric surfaces through the observation of surface dynamics, *Colloids and Surfaces B: Biointerfaces*, **106,** pp. 198-207.
13. Rahul Singhvi, A. K., Gabriel P. Lopez, Gregory N. Stephanopoulos, Daniel I. andC. Wang, G. M. W. a. D. E. I. (1994). Engineering Cell Shape and Function, *Science*, **264,** pp. 696-698.

14. Nguyen, M. (2015). Engineering Thermoswitchable Lithographic Hybrid Gold Nanorods as Plasmonic Devices for Sensing and Active Plasmonics Applications, *ACS Photonics*, **2,** pp. 1199-1208.
15. Nguyen, M. (2015). Tunable Electromagnetic Coupling in Plasmonic Nanostructures Mediated by Thermoresponsive Polymer Brushes, *Langmuir*, **31,** pp. 12830-12837.